IOP PUBLISHING INVERSE PROBLEMS

Inverse Problems **23** (2007) 1215–1228 doi:10.1088/0266-5611/23/3/022

Bioluminescence tomography with optimized optical parameters

Weimin Han[1], **Kamran Kazmi**[1], **Wenxiang Cong**[2] **and Ge Wang**[2]

[1] Department of Mathematics, University of Iowa, Iowa City, IA 52242, USA
[2] Division of Biomedical Imaging, Virginia Tech–Wake Forest University School of Biomedical Engineering and Sciences, VA Polytechnic Institute and State University, Blacksburg, VA 24061, USA

E-mail: whan@math.uiowa.edu, skazmi@math.uiowa.edu, wxcong@gmail.com and ge-wang@ieee.org

Received 7 January 2007, in final form 11 April 2007
Published 17 May 2007
Online at stacks.iop.org/IP/23/1215

Abstract

Bioluminescence tomography (BLT) is a rapidly developing new area of molecular imaging. The goal of BLT is to produce a quantitative reconstruction of a bioluminescent source distribution within a living mouse from bioluminescent signals measured on the body surface of the mouse. While in most BLT studies so far the optical parameters of the key anatomical regions are assumed known from the literature or diffuse optical tomography (DOT), these parameters cannot be very accurate in general. In this paper, we propose and study a new BLT approach that optimizes optical parameters when an underlying bioluminescent source distribution is reconstructed to match the measured data. We prove the solution existence and the convergence of numerical methods. Also, we present numerical results to illustrate the utility of our approach and evaluate its performance.

(Some figures in this article are in colour only in the electronic version)

1. Introduction

A major topic in post-genomic research is studies on relationships between genes and phenotypic expressions. In this regard, mice as human disease models are being extensively studied with various imaging techniques including optical imaging methods. In such optical small animal imaging, mouse organs and tissues are often tagged with fluorescent or bioluminescent probes that help reveal physiological and pathological information at cellular, sub-cellular and molecular levels. Since 2002 our group has pioneered bioluminescence tomography (BLT) systems [7, 20, 21]. Our systems and others prototypes are all demonstrated to enable quantitative 3D reconstructions of internal bioluminescent sources

from bioluminescent measurement on the mouse body surface. Now, BLT has been recognized as a promising area for implementation of the well-known NIH roadmap.

In contrast to the homogeneous mouse model-based method, the major advantage of our BLT approach is the capability of compensating for the heterogeneous optical attenuation maps within a mouse. In the early stage, we segmented a CT scan of a mouse into major anatomical regions, assigned optical parameters to each of the regions according to the literature data, and then performed BLT reconstructions. Quickly, we realized that *in vivo* DOT measurements in combination with the CT scan would produce better results (http://mips.stanford.edu/public/mi_seminar05.adp). Nevertheless, neither of the two ways could produce accurate optical parameters because of the complexity of the biological processes. Hence, it is clear that how to handle this uncertainty for superior imaging performance is a key issue for success of BLT in biomedical applications.

In the conventional BLT problem, the optical parameters are assumed to be known exactly, and the only unknown is the light source function. Such a formulation has been theoretically studied in [12, 21]. In this paper, we upgrade the conventional BLT framework to include the feature of self-adjustment of the optical parameters. In the upgraded BLT framework, we know the optical parameters only approximately, and we want to reconstruct the light source and at the same time determine more accurate values of the optical parameters from the boundary measurements. We form the upgraded BLT framework in section 2 for simultaneous reconstructions of both the underlying bioluminescent source distribution and the involved optical parameters given their approximate initial values and corresponding constraints, and prove the solution existence. In section 3, we discuss numerical approximations and show the convergence of numerical methods. In section 4, we present numerical results to illustrate the utility of our approach and evaluate its performance. Finally, in the last section we discuss relevant issues and conclude the paper.

2. Formulation and solution existence

The bioluminescent photon transport in the biological medium is described by the radiative transfer equation (RTE) [1, 16]. Let Ω be a domain in $\mathbb{R}^3$ with boundary $\Gamma = \partial\Omega$, q be a bioluminescent source function in Ω and $u(\boldsymbol{x}, \boldsymbol{\theta}, t)$ the radiance in $\boldsymbol{\theta} \in S^2$ (S^2: the unit sphere) at $\boldsymbol{x} \in \Omega$. Then the RTE is

$$\frac{1}{c}\frac{\partial u}{\partial t} + \boldsymbol{\theta} \cdot \nabla_{\boldsymbol{x}} u + \mu u = \mu_s \int_{S^2} \eta(\boldsymbol{\theta} \cdot \boldsymbol{\theta}') u(\boldsymbol{x}, \boldsymbol{\theta}', t)\, \mathrm{d}\theta' + q,$$

where c denotes the photon speed, $\mu = \mu_a + \mu_s$ with μ_a and μ_s being the absorption and scattering coefficients, and the scattering kernel η satisfies $\int_{S^2} \eta(\boldsymbol{\theta} \cdot \boldsymbol{\theta}')\, \mathrm{d}\theta' = 1$. Mathematically, BLT is the source inversion problem that is to recover q from optical measurement on the domain boundary Γ, utilizing detailed knowledge of the optical properties of Ω. Note that obtaining the individualized spatially variant optical properties is critical for BLT to work effectively.

Because the RTE is difficult to handle and because in the range of around 600 nm photon scattering outperforms absorption in a mouse, usually a diffusion approximation is used [1, 16]. For the steady state case, we have the following boundary value problem (BVP):

$$-\mathrm{div}(D\nabla u_0) + \mu u_0 = p\chi_{\Omega_0} \quad \text{in } \Omega, \tag{2.1}$$

$$u_0 + 2AD\frac{\partial u_0}{\partial \nu} = g^- \quad \text{on } \Gamma, \tag{2.2}$$

where $u_0(\boldsymbol{x}) = \int_{S^2} u(\boldsymbol{x}, \boldsymbol{\theta})\, \mathrm{d}\theta$, g^- is the incoming flux on Γ and is zero in most applications, $D = 1/[3(\mu_a + \mu_s')]$, $\mu_s' = (1 - \overline{\eta})\mu_s$, $\overline{\eta} = \int_{S^2} \boldsymbol{\theta} \cdot \boldsymbol{\theta}' \eta(\boldsymbol{\theta} \cdot \boldsymbol{\theta}')\, \mathrm{d}\theta'$, and $p(\boldsymbol{x}) = \int_{S^2} q(\boldsymbol{x}, \boldsymbol{\theta})\, \mathrm{d}\theta/(4\pi)$. The appearance of the parameter A in the boundary condition (2.2) is to incorporate diffuse boundary reflection arising from a refractive index mismatch between the body Ω and the surrounding medium. We have

$$A = (1 + R)/(1 - R), \tag{2.3}$$

with R being a directionally varying refraction parameter. The set Ω_0 is a measurable subset of Ω ($\Omega_0 = \Omega$ is allowed), χ_{Ω_0} is the characteristic function of Ω_0, i.e., its value is 1 in Ω_0, and is 0 in $\Omega \backslash \Omega_0$. Thus, the light source exists only in Ω_0, known as the permissible region. Note that the subset Ω_0 itself can be the union of a collection of disjoint subsets of Ω. The measurement is

$$\tilde{f} = -D \frac{\partial u}{\partial \nu} \quad \text{on } \Gamma. \tag{2.4}$$

Then, the BLT problem is to find a source function q_0 given g^- and g such that (2.1), (2.2) and (2.4) are satisfied. We call this the pointwise formulation. The pointwise formulation is ill posed: (1) in general, there are infinite many solutions; (2) when the form of the source function is specified, generally there are no solutions. Moreover, the source function does not depend continuously on the data.

To avoid complicated subscripts, we simplify the notation by expressing the new BLT approach as the determination of the parameters D, μ, and a source function p of the boundary value problem

$$-\mathrm{div}\,(D\nabla u) + \mu u = p\chi_{\Omega_0} \quad \text{in } \Omega, \tag{2.5}$$

$$u + 2AD \frac{\partial u}{\partial \nu} = 0 \quad \text{on } \Gamma, \tag{2.6}$$

such that its solution u takes on the measured flux quantity

$$\tilde{f} = -D \frac{\partial u}{\partial \nu} = \frac{1}{2A} u \qquad \text{on } \Gamma_0 \tag{2.7}$$

and $D \approx D^{(0)}$, $\mu \approx \mu^{(0)}$ with given $D^{(0)}$ and $\mu^{(0)}$. Here $D = [3(\mu + \mu')]^{-1}$, μ and μ' are absorption and reduced scattering coefficients, respectively, and $\Gamma_0 \subset \Gamma$. Note that we allow the measurement to be available only on a proper part Γ_0 of the boundary Γ.

In practical applications of BLT, the coefficients D and μ are piecewise constants. In other words, the biological medium $\overline{\Omega}$ consists of a finite number (M) of subdomains $\overline{\Omega_m}$, $1 \leqslant m \leqslant M$, such that $\overline{\Omega} = \cup_{m=1}^{M} \overline{\Omega_m}$, $\Omega_m \cap \Omega_n = \emptyset$ for $m \neq n$, and

$$D(\boldsymbol{x}) = D_m, \qquad \mu(\boldsymbol{x}) = \mu_m, \qquad \boldsymbol{x} \in \Omega_m, \quad 1 \leqslant m \leqslant M. \tag{2.8}$$

Moreover, based on past experimental results, the coefficients D and μ are expected to be close to known piecewise constant functions $D^{(0)}$ and $\mu^{(0)}$:

$$D^{(0)}(\boldsymbol{x}) = D_m^{(0)}, \qquad \mu^{(0)}(\boldsymbol{x}) = \mu_m^{(0)}, \qquad \boldsymbol{x} \in \Omega_m, \quad 1 \leqslant m \leqslant M,$$

with $D_m^{(0)} > 0$ and $\mu_m^{(0)} > 0$, $1 \leqslant m \leqslant M$.

For the given data, we assume $\Omega \subset \mathbb{R}^d$ ($d \leqslant 3$) is a non-empty, open, bounded set with a Lipschitz boundary Γ and Γ_0 is a Lipschitz part of Γ. We also assume $\Omega_0 \subset \Omega$ is a non-empty, open, bounded set with a Lipschitz boundary. Denote $f = 2A\tilde{f}$, and assume $f \in L^2(\Gamma_0)$. Also assume $A > 0$ and $A^{-1} \in L^\infty(\Gamma)$; these conditions are always satisfied in applications.

Suppose we seek the source function p in a closed convex subset Q_p of the space $L^2(\Omega_0)$. Examples include $Q_p = L^2(\Omega_0)$, or the subset of $L^2(\Omega_0)$ of non-negatively valued functions,

or a finite-dimensional subspace or subset of linear combinations of specified functions such as the characteristic functions of certain subsets of Ω. Furthermore, for given non-negative numbers $r_{D,m} \in \left[0, D_m^{(0)}\right)$ and $r_{\mu,m} \in \left[0, \mu_m^{(0)}\right)$, $1 \leqslant m \leqslant M$, we introduce the sets

$$Q_D = \left\{D \mid D|_{\Omega_m} = D_m \in \mathbb{R}, \left|D_m - D_m^{(0)}\right| \leqslant r_{D,m}, 1 \leqslant m \leqslant M\right\}, \tag{2.9}$$

$$Q_\mu = \left\{\mu \mid \mu|_{\Omega_m} = \mu_m \in \mathbb{R}, \left|\mu_m - \mu_m^{(0)}\right| \leqslant r_{\mu,m}, 1 \leqslant m \leqslant M\right\}. \tag{2.10}$$

Note that it is allowed to have $r_{D,m} = 0$ or $r_{\mu,m} = 0$ for some values of m. In such a situation, we have $D_m = D_m^{(0)}$ or $\mu_m = \mu_m^{(0)}$, and these parameters are no longer unknowns of the problem. Denote the admissible set

$$Q_{ad} = Q_D \times Q_\mu \times Q_p.$$

We denote by $u = u(D, \mu, p) \in V \equiv H^1(\Omega)$ the solution of the boundary value problem

$$\int_\Omega (D\nabla u \cdot \nabla v + \mu u v)\,\mathrm{d}x + \int_\Gamma \frac{1}{2A} u v\,\mathrm{d}s = \int_{\Omega_0} p v\,\mathrm{d}x \qquad \forall\, v \in V. \tag{2.11}$$

By the well-known Lax–Milgram lemma (e.g. [2, 11]), due to the assumptions made on the data, for any $(D, \mu, p) \in Q_{ad}$, the solution $u(D, \mu, p)$ exists and is unique.

For $\varepsilon_D \geqslant 0, \varepsilon_\mu \geqslant 0$ and $\varepsilon_p \geqslant 0$, denote $\varepsilon = (\varepsilon_D, \varepsilon_\mu, \varepsilon_p)$. Following the idea of regularization [19, 10], let

$$\begin{aligned} J_\varepsilon(D, \mu, p) = \tfrac{1}{2}\big[&\|u(D, \mu, p) - f\|^2_{L^2(\Gamma_0)} + \varepsilon_D \|D - D^{(0)}\|^2_{L^2(\Omega)} \\ &+ \varepsilon_\mu \|\mu - \mu^{(0)}\|^2_{L^2(\Omega)} + \varepsilon_p \|p\|^2_{L^2(\Omega_0)}\big] \end{aligned} \tag{2.12}$$

and introduce the following problem for simultaneous determination of the parameters D and μ, and the source function p:

$$\inf\{J_\varepsilon(D, \mu, p) \mid (D, \mu, p) \in Q_{ad}\}. \tag{2.13}$$

Theorem 2.1. *Assume $\varepsilon_p > 0$ or $Q_p \subset L^2(\Omega_0)$ is bounded. Then problem (2.13) has a solution.*

Proof. Denote by $\alpha \geqslant 0$ the infimum value of (2.13). By the definition of infimum, there is a sequence $\{(D_n, \mu_n, p_n)\}_{n\geqslant 1} \subset Q_{ad}$ such that

$$J_\varepsilon(D_n, \mu_n, p_n) \to \alpha \qquad \text{as} \quad n \to \infty.$$

Because of the compactness of the intervals $\left[D_m^{(0)} - r_{D,m}, D_m^{(0)} + r_{D,m}\right]$ and $\left[\mu_m^{(0)} - r_{\mu,m}, \mu_m^{(0)} + r_{\mu,m}\right]$, $1 \leqslant m \leqslant M$, there are a subsequence of $\{n\}$, still denoted by $\{n\}$, $D_\infty \in Q_D$ and $\mu_\infty \in Q_\mu$ such that

$$D_n \to D_\infty, \qquad \mu_n \to \mu_\infty \qquad \text{in } L^\infty(\Omega), \qquad \text{as} \quad n \to \infty.$$

Under the assumption that $\varepsilon > 0$ or $Q_p \subset L^2(\Omega_0)$ is bounded, $\{p_n\}$ is a bounded sequence in $L^2(\Omega_0)$. Therefore, resorting to a further subsequence if necessary, there is $p_\infty \in Q_p$ such that we have the weak convergence

$$p_n \rightharpoonup p_\infty \qquad \text{in } L^2(\Omega_0), \qquad \text{as} \quad n \to \infty.$$

Write $u_n = u(D_n, \mu_n, p_n)$. Then it is easy to know that the sequence $\{\|u_n\|_V\}$ is bounded. So again resorting to a further subsequence if necessary, there is $u_\infty \in V$ such that

$$u_n \rightharpoonup u_\infty \qquad \text{in } V, \qquad \text{as} \quad n \to \infty.$$

This in particular implies $u_n \to u$ in $L^2(\Gamma)$.

Let $n \to \infty$ in

$$\int_\Omega (D_n \nabla u_n \cdot \nabla v + \mu_n u_n v)\,\mathrm{d}x + \int_\Gamma \frac{1}{2A} u_n v\,\mathrm{d}s = \int_{\Omega_0} p_n v\,\mathrm{d}x \qquad \forall\, v \in V$$

to get

$$\int_\Omega (D_\infty \nabla u_\infty \cdot \nabla v + \mu_\infty u_\infty v)\,dx + \int_\Gamma \frac{1}{2A} u_\infty v\,ds = \int_{\Omega_0} p_\infty v\,dx \qquad \forall\, v \in V. \tag{2.14}$$

Hence, $u_\infty = u(D_\infty, \mu_\infty, p_\infty)$. Moreover,

$$J_\varepsilon(D_\infty, \mu_\infty, p_\infty) \leqslant \lim_{n\to\infty} J_\varepsilon(D_n, \mu_n, p_n) = \alpha.$$

Therefore, $(D_\infty, \mu_\infty, p_\infty) \in Q_{ad}$ is a solution of problem (2.13). □

This theorem states that problem (2.13) has solutions. The next result provides a necessary condition for a solution of problem (2.13).

Proposition 2.2. *Let $(D_\infty, \mu_\infty, p_\infty) \in Q_{ad}$ be a solution of problem (2.13) and denote $u_\infty = u(D_\infty, \mu_\infty, p_\infty)$. Then*

$$\begin{aligned}(u_\infty - f, w_\infty)_{L^2(\Gamma_0)} &+ \varepsilon_D (D_\infty - D^{(0)}, D - D_\infty)_{L^2(\Omega)} + \varepsilon_\mu (\mu_\infty - \mu^{(0)}, \mu - \mu_\infty)_{L^2(\Omega)} \\ &+ \varepsilon_p (p_\infty, p - p_\infty)_{L^2(\Omega_0)} \geqslant 0 \qquad \forall\, (D, \mu, p) \in Q_{ad},\end{aligned} \tag{2.15}$$

where $w_\infty = w_\infty(D - D_\infty, \mu - \mu_\infty, p - p_\infty) \in V$ is the solution of the boundary value problem

$$\begin{aligned}\int_\Omega (D_\infty \nabla w_\infty \cdot \nabla v + \mu_\infty w_\infty v)\,dx + \int_\Gamma \frac{1}{2A} w_\infty v\,ds &= \int_{\Omega_0} (p - p_\infty) v\,dx \\ - \int_\Omega [(D - D_\infty)\nabla u_\infty \cdot \nabla v + (\mu - \mu_\infty) u_\infty v]\,dx &\qquad \forall\, v \in V.\end{aligned} \tag{2.16}$$

Proof. Define $u_t \in V$ as the solution of the boundary value problem

$$\begin{aligned}\int_\Omega \big[(D_\infty + t(D - D_\infty))\nabla u_t \cdot \nabla v + (\mu_\infty + t(\mu - \mu_\infty)) u_t v\big]\,dx + \int_\Gamma \frac{1}{2A} u_t v\,ds \\ = \int_{\Omega_0} (p_\infty + t(p - p_\infty)) v\,dx \qquad \forall\, v \in V.\end{aligned} \tag{2.17}$$

Consider the function

$$\begin{aligned}g(t) = \tfrac{1}{2}\big[\|u_t - f\|^2_{L^2(\Gamma_0)} &+ \varepsilon_D \|D_\infty + t(D - D_\infty) - D^{(0)}\|^2_{L^2(\Omega)} + \varepsilon_\mu \|\mu_\infty + t(\mu - \mu_\infty) \\ &- \mu^{(0)}\|^2_{L^2(\Omega)} + \varepsilon_p \|p_\infty + t(p - p_\infty)\|^2_{L^2(\Omega_0)}\big], \qquad 0 \leqslant t \leqslant 1.\end{aligned}$$

Then $g(t)$ has its minimum at $t = 0$ for $t \in [0, 1]$, and so

$$g'(0+) \geqslant 0.$$

Now

$$\begin{aligned}g'(t) = \left(u_t - f, \frac{\partial u_t}{\partial t}\right)_{L^2(\Gamma_0)} &+ \varepsilon_D (D_\infty + t(D - D_\infty) - D^{(0)}, D - D_\infty)_{L^2(\Omega)} \\ &+ \varepsilon_\mu (\mu_\infty + t(\mu - \mu_\infty) - \mu^{(0)}, \mu - \mu_\infty)_{L^2(\Omega)} \\ &+ \varepsilon_p\, (p_\infty + t(p - p_\infty), p - p_\infty)_{L^2(\Omega_0)}\,.\end{aligned}$$

Differentiate (2.17) with respect to t to obtain

$$\begin{aligned}\int_\Omega \left[(D_\infty + t(D - D_\infty))\,\nabla \frac{\partial u_t}{\partial t} \cdot \nabla v + (\mu_\infty + t(\mu - \mu_\infty))\,\frac{\partial u_t}{\partial t} v\right] dx + \int_\Gamma \frac{1}{2A} \frac{\partial u_t}{\partial t} v\,ds \\ = \int_{\Omega_0} (p - p_\infty) v\,dx - \int_\Omega [(D - D_\infty)\nabla u_t \cdot \nabla v + (\mu - \mu_\infty) u_t v]\,dx \quad \forall\, v \in V.\end{aligned} \tag{2.18}$$

Obviously, $u_t : t \in [0, 1] \to V$ is continuous as a function of t. So $u_t \to u_\infty$ in V as $t \to 0+$. Let $t \to 0+$ in (2.18) to obtain (2.16) for

$$w_\infty = \lim_{t\to 0+} \frac{\partial u_t}{\partial t}.$$

Thus,

$$g'(0+) = (u_\infty - f, w_\infty)_{L^2(\Gamma_0)} + \varepsilon_D(D_\infty - D^{(0)}, D - D_\infty)_{L^2(\Omega)} + \varepsilon_\mu(\mu_\infty - \mu^{(0)}, \mu - \mu_\infty)_{L^2(\Omega)} + \varepsilon_p(p_\infty, p - p_\infty)_{L^2(\Omega_0)} \geqslant 0,$$

i.e., (2.15) holds. □

Solution uniqueness for problem (2.13) is a difficult question, even in the case $\varepsilon_p > 0$. In this regard, the above necessary condition of a solution may be useful. Since a solution to the problem with $\varepsilon_p > 0$ and $r_{D,m} = r_{\mu,m} = 0$ for $1 \leqslant m \leqslant M$ is unique and depends continuously on the data [12], we expect a solution to problem (2.13) for $\varepsilon_p > 0$ is unique when $r_{D,m}$ and $r_{\mu,m}$, $1 \leqslant m \leqslant M$, are assumed small and changes of the optical parameters are restricted in certain ways.

3. Numerical approximations

We now turn to a discussion of numerical solutions of problem (2.13). For simplicity in discussion, we assume Ω_m, $1 \leqslant m \leqslant M$, and Ω_0 to be unions of polygonal (for $d = 2$) or polyhedral (for $d = 3$) domains. Let $\{\mathcal{T}\}_{h>0}$ (h: mesh size) be a regular family of finite element partitions of $\overline{\Omega}$ that respect the domain splitting $\overline{\Omega} = \cup_{m=1}^{M} \overline{\Omega_m}$, i.e. if one side of an element $K \in \mathcal{T}_h$ intersects the boundary of a region Ω_m at more than one point, then the entire element side lies on the boundary of Ω_m. For each triangulation $\mathcal{T}_h = \{K\}$, let $V^h \subset V$ be the corresponding finite element space of continuous piecewise linear functions. Let $\{\mathcal{T}_{H,\Omega_0}\}$ (H: mesh size) be a regular family of finite element partitions of $\overline{\Omega_0}$. Note that the partitions $\{\mathcal{T}_h\}$ and $\{\mathcal{T}_{H,\Omega_0}\}$ are allowed to be independent of each other. Let Q_p^H be the piecewise constant finite element subset approximating Q_p. Then Q_p^H is non-empty, closed and convex, and we have the property

$$\forall\, q \in Q_p, \qquad \exists q^H \in Q_p^H \text{ such that } \|q^H - q\|_{L^2(\Omega_0)} \to 0 \quad \text{as } H \to 0.$$

Indeed, we may simply take q^H to be the piecewise average of q over $\mathcal{T}_{H,\Omega_0}$. Denote $u^{hH} = u^{hH}(D, \mu, p^H) \in V^h$ for the solution of the problem

$$\int_\Omega (D\nabla u^{hH} \cdot \nabla v^h + \mu u^{hH} v^h)\,\mathrm{d}x + \int_\Gamma \frac{1}{2A} u^{hH} v^h\,\mathrm{d}s = \int_{\Omega_0} p^H v^h\,\mathrm{d}x \qquad \forall\, v^h \in V^h. \tag{3.1}$$

By the Lax–Milgram lemma, the solution u^{hH} exists and is unique. Let

$$J_\varepsilon^{hH}(D, \mu, p^H) = \tfrac{1}{2}\big[\|u^{hH}(D, \mu, p^H) - f\|_{L^2(\Gamma_0)}^2 + \varepsilon_D\|D - D^{(0)}\|_{L^2(\Omega)}^2 + \varepsilon_\mu\|\mu - \mu^{(0)}\|_{L^2(\Omega)}^2 + \varepsilon_p\|p^H\|_{L^2(\Omega_0)}^2\big]. \tag{3.2}$$

Denote $Q_{ad}^H = Q_D \times Q_\mu \times Q_p^H$. We then introduce the following discretization of problem (2.13):

$$\inf\big\{J_\varepsilon^{hH}(D, \mu, p^H) \,\big|\, (D, \mu, p^H) \in Q_{ad}^H\big\}. \tag{3.3}$$

Like for problem (2.13), under the assumption of theorem 2.1, there is a solution to the discrete problem (3.3). Denote by α^{hH} the infimum value of (3.3). Let us first show the following convergence result on the discrete minimum values.

Theorem 3.1. *As $h, H \to 0$, $\alpha^{hH} \to \alpha$.*

Proof. Let $(D_\infty, \mu_\infty, p_\infty) \in Q_{ad}$ be a solution of (2.13). Choose $p_\infty^H \in Q_p^H$ such that

$$p_\infty^H \to p_\infty \qquad \text{in } L^2(\Omega_0), \qquad \text{as } H \to 0. \tag{3.4}$$

Note that $u_\infty = u(D_\infty, \mu_\infty, p_\infty)$ satisfies (2.14). Denote $u_\infty^{hH} = u^{hH}\big(D_\infty, \mu_\infty, p_\infty^H\big)$. Then by (3.1),

$$\int_\Omega \big(D_\infty \nabla u_\infty^{hH} \cdot \nabla v^h + \mu_\infty u_\infty^{hH} v^h\big)\,\mathrm{d}x + \int_\Gamma \frac{1}{2A} u_\infty^{hH} v^h \mathrm{d}s = \int_{\Omega_0} p_\infty^H v^h \mathrm{d}x \qquad \forall\, v^h \in V^h.$$

Subtract this from (2.14),

$$\int_\Omega \big[D_\infty \nabla\big(u_\infty - u_\infty^{hH}\big) \cdot \nabla v^h + \mu_\infty\big(u_\infty - u_\infty^{hH}\big)v^h\big]\,\mathrm{d}x + \int_\Gamma \frac{1}{2A}\big(u_\infty - u_\infty^{hH}\big)v^h \mathrm{d}s$$
$$= \int_{\Omega_0} \big(p_\infty - p_\infty^H\big)\, v^h \mathrm{d}x \qquad \forall\, v^h \in V^h.$$

From this error relation, we obtain the following result through a standard argument:

$$\big\|u_\infty - u_\infty^{hH}\big\|_V \leqslant c\left[\inf_{v^h \in V^h} \|u_\infty - v^h\|_V + \big\|p_\infty - p_\infty^H\big\|_{L^2(\Omega_0)}\right] \to 0 \qquad \text{as} \quad h, H \to 0.$$

Since $\alpha^{hH} \leqslant J_\varepsilon^{hH}\big(D_\infty, \mu_\infty, p_\infty^H\big)$, we have

$$\limsup_{h,H\to 0} \alpha^{hH} \leqslant \lim_{h,H\to 0} J_\varepsilon^{hH}\big(D_\infty, \mu_\infty, p_\infty^H\big) = \alpha. \tag{3.5}$$

Conversely, any sequence $\{(D^{hH}, \mu^{hH}, p^{hH})\} \subset Q_{ad}^H$ contains a subsequence, still denoted by $\{(D^{hH}, \mu^{hH}, p^{hH})\}$, such that

$$D^{hH} \to D, \qquad \mu^{hH} \to \mu \qquad \text{in } L^\infty(\Omega), \qquad p^{hH} \rightharpoonup p \qquad \text{in } L^2(\Omega_0), \qquad \text{as } h, H \to 0 \tag{3.6}$$

for some $D \in Q_D$, $\mu \in Q_\mu$, and $p \in Q_p$. Let us show that

$$u^{hH}(D^{hH}, \mu^{hH}, p^{hH}) \rightharpoonup u(D, \mu, p) \quad \text{in } V, \text{ as } h, H \to 0.$$

First, by (3.1)

$$\int_\Omega (D^{hH} \nabla u^{hH} \cdot \nabla v^h + \mu^{hH} u^{hH} v^h)\,\mathrm{d}x + \int_\Gamma \frac{1}{2A} u^{hH} v^h\,\mathrm{d}s = \int_{\Omega_0} p^{hH} v^h\,\mathrm{d}x \quad \forall\, v^h \in V^h. \tag{3.7}$$

It can be shown that $\{\|u^{hH}\|_V\}$ is uniformly bounded, independent of h and H. So there exists a subsequence $\{u^{hH}\}$, still denoted by $\{u^{hH}\}$, and $u \in V$ such that $u^{hH} \rightharpoonup u$ in V. Taking $h, H \to 0$ along this subsequence in (3.7) to get

$$\int_\Omega (D\nabla u \cdot \nabla v + \mu u v)\,\mathrm{d}x + \int_\Gamma \frac{1}{2A} u v\,\mathrm{d}s = \int_{\Omega_0} p v\,\mathrm{d}x \qquad \forall\, v \in V,$$

i.e. the limit $u = u(D, \mu, p)$. Since the limit u is unique, the entire sequence converges: $u^{hH} \rightharpoonup u$ in V as $h, H \to 0$. A consequence of this is $u^{hH}(D^{hH}, \mu^{hH}, p^{hH}) \to u(D, \mu, p)$ in $L^2(\Gamma)$. Hence,

$$J_\varepsilon(D, \mu, p) \leqslant \liminf_{h,H\to 0} J_\varepsilon^{hH}(D^{hH}, \mu^{hH}, p^{hH}) \tag{3.8}$$

and so

$$\alpha \leqslant \liminf_{h,H\to 0} \alpha^{hH}. \tag{3.9}$$

Combining (3.5) and (3.9), we complete the proof. □

Thus, the discrete minimum objective function values converge to the original minimum objective function value.

We also have convergence of the numerical solutions.

Theorem 3.2. *Any sequence of solutions of problem (3.3) contains a subsequence converging to a solution of problem (2.13). Moreover, any converging sequence of solutions of problem (3.3) converges to a solution of problem (2.13).*

Proof. Let $\{(D^{hH}, \mu^{hH}, p^{hH})\}$ be a sequence of solutions of (3.3). Then as in the second part of the proof of theorem 3.1, there is a subsequence, still denoted as $\{(D^{hH}, \mu^{hH}, p^{hH})\}$, and $(D, \mu, p) \in Q_{ad}$ such that (3.6) holds. Let $(D_\infty, \mu_\infty, p_\infty)$ be a solution of (2.13), and choose $p_\infty^H \in Q_p^H$ satisfying (3.4). Then by (3.5),

$$J_\varepsilon^{hH}\big(D_\infty, \mu_\infty, p_\infty^H\big) \to J_\varepsilon(D_\infty, \mu_\infty, p_\infty),$$

and by (3.8),

$$\limsup_{h,H\to 0} J_\varepsilon^{hH}(D^{hH}, \mu^{hH}, p^{hH}) \geqslant J_\varepsilon(D, \mu, p).$$

Now

$$J_\varepsilon^{hH}(D^{hH}, \mu^{hH}, p^{hH}) \leqslant J_\varepsilon^{hH}\big(D_\infty, \mu_\infty, p_\infty^H\big).$$

Combining these relations,

$$J_\varepsilon(D, \mu, p) \leqslant J_\varepsilon(D_\infty, \mu_\infty, p_\infty),$$

i.e., the limit (D, μ, p) is a solution of (2.13).

The above argument also proves the second part of the theorem. □

This result shows that we can get arbitrarily accurate approximation of a solution of problem (2.13) from any sequence of discrete solutions when the finite element mesh sizes go to zero.

4. Numerical examples

In this section, we present numerical results from two examples for simulation of the upgraded BLT model. In the first example, we examine the convergence behaviour of the numerical solution as the mesh size is made progressively smaller. In the second example, we consider a more realistic problem setting to assess the practicality of the proposed approach.

Example 4.1. We demonstrate the feasibility of the numerical method discussed in section 3 through a simple two-dimensional sample problem described by the boundary value problem (2.5)–(2.6) with the measurement (2.7), where A is given by (2.3) for

$$R = -1.4399\eta^{-2} + 0.7099\eta^{-1} + 0.6681 + 0.0636\eta, \tag{4.1}$$

with the refractive index $\eta = 1.33$. Let $\Omega = (0, 1) \times (0, 1)$ be the domain. The closed region $\overline{\Omega}$ is divided into four subregions $\overline{\Omega_m}$, $1 \leqslant m \leqslant 4$, with $\Omega_1 = (0, 0.5) \times (0, 0.5)$, $\Omega_2 = (0.5, 1) \times (0, 0.5)$, $\Omega_3 = (0, 0.5) \times (0.5, 1)$, and $\Omega_4 = (0.5, 1) \times (0.5, 1)$; see figure 1. In each subregion Ω_m, $1 \leqslant m \leqslant 4$, the values of the optical parameters D and μ are constant. The true values of μ and D are taken as

$$(\mu, D) = \begin{cases} (0.02, 0.3268) & \text{in} \quad \Omega_1, \\ (0.14, 0.1916) & \text{in} \quad \Omega_2, \\ (0.01, 0.5464) & \text{in} \quad \Omega_3, \\ (0.08, 0.2415) & \text{in} \quad \Omega_4. \end{cases}$$

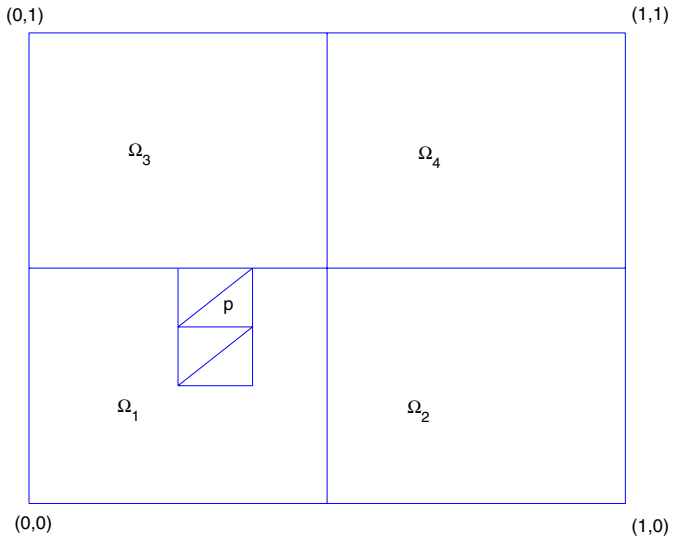

Figure 1. The domain Ω.

As their approximate values, we choose

$$(\mu^{(0)}, D^{(0)}) = \begin{cases} (0.05, 0.6) & \text{in} \quad \Omega_1, \\ (0.1, 0.12) & \text{in} \quad \Omega_2, \\ (0.035, 0.35) & \text{in} \quad \Omega_3, \\ (0.05, 0.6) & \text{in} \quad \Omega_4. \end{cases}$$

The bounds in defining the sets Q_D of (2.9) and Q_μ of (2.10) are $r_D = [0.5, 0.1, 0.3, 0.5]^T$, $r_\mu = [0.04, 0.05, 0.03, 0.04]^T$, respectively. The regularization parameters are $\varepsilon_D = 10^{-4}$, $\varepsilon_\mu = 10^{-4}$ and $\varepsilon_p = 10^{-7}$. The source p is placed in the region $\Omega_0 = (0.25, 0.375) \times (0.25, 0.5)$, and the true source function p is taken to be 10. We divide $\overline{\Omega_0}$ into four congruent triangles, labelled upward; the admissible set Q_p^H consists of correspondingly piecewise constant functions.

We use linear elements on uniform triangular partitions of the domain Ω. The uniform meshes are obtained by dividing the interval $[0, 1]$ into $1/h$ equal parts in both x and y directions. We start with an initial mesh with $h = 1/8$ and then successively halve h to obtain more refined meshes. We take the numerical solution of the boundary value problem (2.11) computed using the exact values of D, μ and p, and on the mesh with mesh size $h = 1/512$ as the true solution and use it to obtain the measured quantity f on $\Gamma_0 = \Gamma$.

The numerical solutions of problem (3.3) are then computed using this value of f on the meshes with the mesh size $h = 1/8, 1/16, 1/32, 1/64$ using Matlab and its optimization toolbox. The optimization part is terminated when the change in the relative function value is less than the tolerance FunTol $= 10^{-8}$.

Note that the numerical solutions of problem (3.3) depend on the regularization parameters ε_D, ε_μ and ε_p. Also note that H is fixed in this example. For these reasons, we denote the numerical solutions by D_ε^h, μ_ε^h and p_ε^h. Computed values of D_ε^h, μ_ε^h and p_ε^h for various choices of h along with the norm of errors between exact values and the computed values are given in tables 1–3. The plots of the norm of the errors are given in figures 2–4.

Example 4.2. To demonstrate the feasibility of the proposed numerical reconstruction method for a more realistic problem, we consider a heterogeneous phantom occupying a circle of

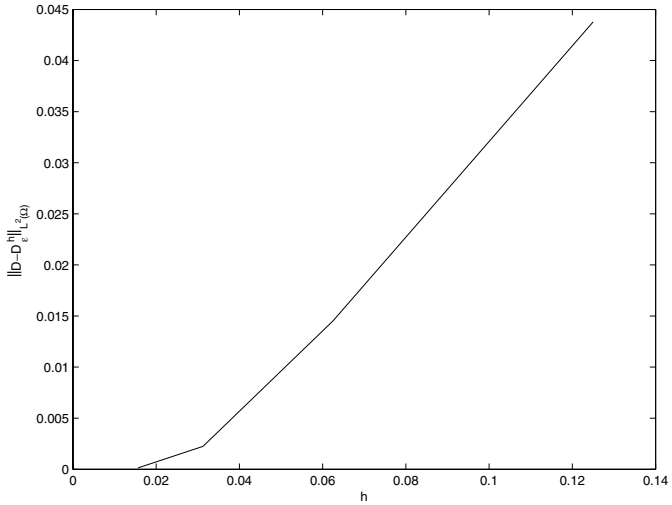

Figure 2. Plot of the error $\|D - D_\varepsilon^h\|_{L^2(\Omega)}$.

Table 1. Numerical results for D_ε^h.

	Ω_1	Ω_2	Ω_3	Ω_4	$\|D - D_\varepsilon^h\|_{L^2(\Omega)}$
$h = 1/8$	0.3642	0.1906	0.5517	0.2436	4.3792×10^{-2}
$h = 1/16$	0.3356	0.1905	0.5509	0.2439	1.4525×10^{-2}
$h = 1/32$	0.3290	0.1906	0.5463	0.2427	2.2364×10^{-3}
$h = 1/64$	0.3273	0.1911	0.5465	0.2416	1.3788×10^{-4}

Table 2. Numerical results for μ_ε^h.

	Ω_1	Ω_2	Ω_3	Ω_4	$\|\mu - \mu_\varepsilon^h\|_{L^2(\Omega)}$
$h = 1/8$	0.0763	0.1222	0.0050	0.0900	4.3532×10^{-2}
$h = 1/16$	0.0424	0.1304	0.0099	0.0900	2.2669×10^{-2}
$h = 1/32$	0.0182	0.1321	0.0050	0.0845	1.0210×10^{-2}
$h = 1/64$	0.0179	0.1361	0.0091	0.0802	6.7959×10^{-3}

Table 3. Numerical results for p_ε^h.

	Element 1	Element 2	Element 3	Element 4	$\|p - p_\varepsilon^h\|_{L^2(\Omega_0)}$
$h = 1/8$	8.8623	10.5454	11.5751	9.8358	1.7897×10^{-1}
$h = 1/16$	9.8603	10.2733	10.4859	9.7880	5.4145×10^{-2}
$h = 1/32$	9.9007	9.9788	10.2561	9.7022	3.5857×10^{-2}
$h = 1/64$	9.9770	10.0012	10.2276	9.6908	3.3992×10^{-2}

radius 1 cm centred at the origin. The unit circle is split into four annular regions Ω_1, Ω_2, Ω_3 and Ω_4, defined by circles of radii 1.0, 0.9, 0.8 and 0.7, all centred at the origin. See figure 5 for the geometric setting. A light source with power of 6.0 nW is uniformly distributed

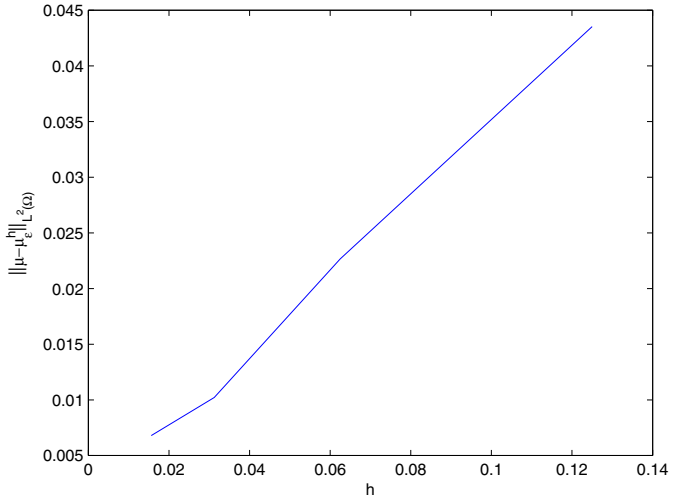

Figure 3. Plot of the error $\|\mu - \mu_\varepsilon^h\|_{L^2(\Omega)}$.

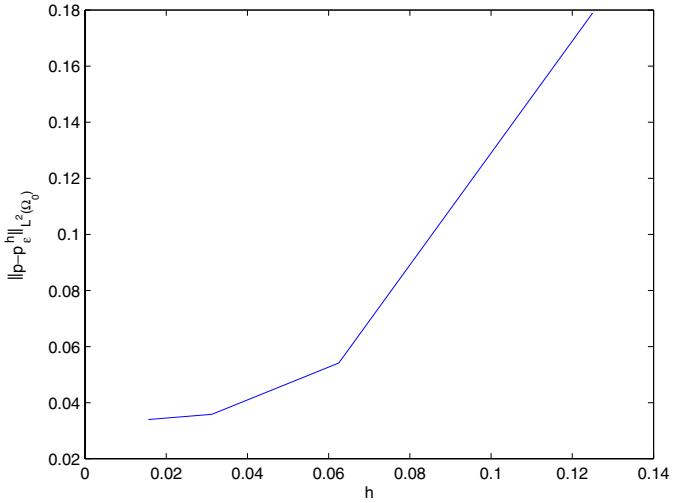

Figure 4. Plot of the error $\|p - p_\varepsilon^h\|_{L^2(\Omega_0)}$.

on a circle with radius 0.03 cm centred at $(0, 0.6)$. The true optical parameters (μ, D) (unit: $(\mathrm{cm}^{-1}, \mathrm{cm})$) are taken to be

$$(\mu, D) = \begin{cases} (0.6, 0.042\,735) & \text{in} \quad \Omega_1, \\ (0.1, 0.128\,21) & \text{in} \quad \Omega_2, \\ (1.2, 0.024\,331) & \text{in} \quad \Omega_3, \\ (0.8, 0.033\,67) & \text{in} \quad \Omega_4. \end{cases}$$

The phantom is discretized into 5400 triangle elements with 2791 nodes. The 180 outer boundary nodes are used to record photon flux density on the outer boundary. In practice, the measurement modality can be realized using non-contact imaging, which is able to collect

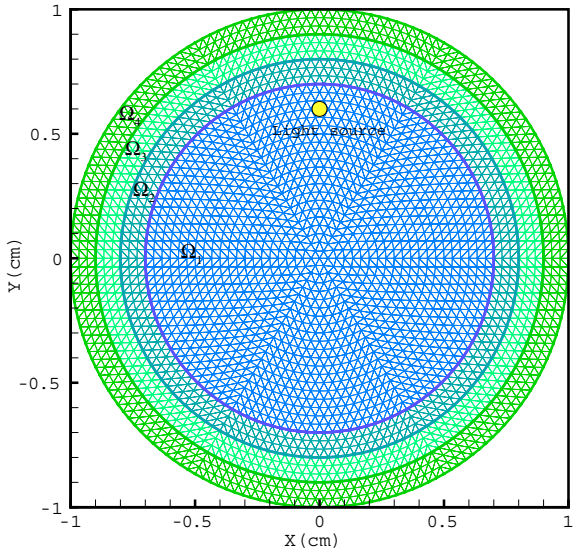

Figure 5. Geometry of phantom.

large data sets by using highly sensitive charge-coupled device (CCD) cameras as detectors. Boundary reflection coefficient R is computed using (4.1), and in this example, we choose $\eta = 1.37$ for the refractive index. As known approximate values, we take

$$(\mu^{(0)}, D^{(0)}) = \begin{cases} (0.48, 0.034\,188) & \text{in} \quad \Omega_1, \\ (0.08, 0.102\,57) & \text{in} \quad \Omega_2, \\ (0.96, 0.019\,465) & \text{in} \quad \Omega_3, \\ (0.64, 0.026\,936) & \text{in} \quad \Omega_4. \end{cases}$$

In (2.9) and (2.10), the sets Q_D and Q_μ are defined through specifying values of the radii for r_D and r_μ. All the theoretical results in previous sections are valid also for the case where Q_D and Q_m are specified by bounded closed intervals on the positive axis for each component of r_D and r_μ. In this example, we specify

$$\mu_1 \in [0.42, 0.78], \qquad \mu_2 \in [0.07, 0.13], \qquad \mu_3 \in [0.84, 1.56], \qquad \mu_4 \in [0.56, 1.04];$$
$$D_1 \in [0.029\,915, 0.055\,556], \qquad D_2 \in [0.089\,744, 0.166\,67],$$
$$D_3 \in [0.017\,032, 0.031\,63], \qquad D_4 \in [0.023\,569, 0.043\,771]$$

in defining Q_μ and Q_D. We choose the regularization parameters to be $\varepsilon_D = 10^{-5}$, $\varepsilon_\mu = 10^{-5}$ and $\varepsilon_p = 10^{-7}$. The measured data on the boundary are generated from the solution of the boundary value problem (2.5)–(2.7), corrupted by 5% Gaussian noise, as shown in figure 6. The permissible region Ω_0 is set to a circle with radius of 0.06 cm centred at $(0, 0.6)$. Then we solve the reconstruction problem (3.3) to identify the optical parameters and light source distribution. Again we use the Matlab optimization toolbox in implementation.

The reconstructed coefficients for (μ, D) are

$$\left(\mu_\varepsilon^h, D_\varepsilon^h\right) = \begin{cases} (0.624\,21, 0.047\,11) & \text{in} \quad \Omega_1, \\ (0.0949, 0.105\,71) & \text{in} \quad \Omega_2, \\ (1.3079, 0.019\,465) & \text{in} \quad \Omega_3, \\ (0.816\,04, 0.027\,086) & \text{in} \quad \Omega_4. \end{cases}$$

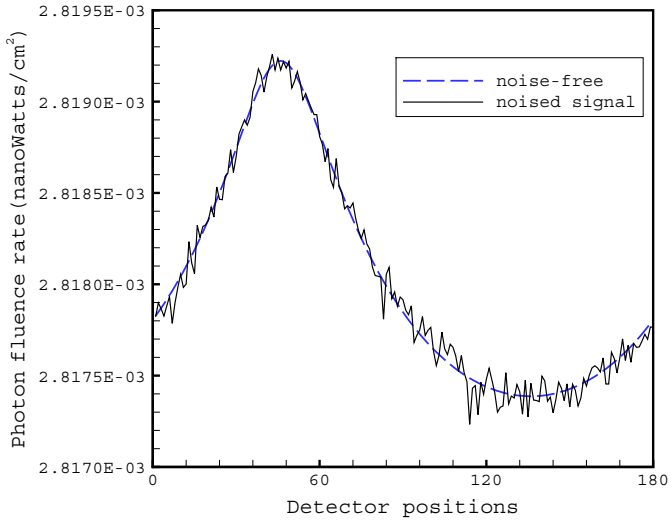

Figure 6. Measurement data.

The maximum relative errors of absorption coefficients between true and calculated optical parameters are less than 9%, the maximum relative errors of the diffusion coefficients between true and calculated optical parameters are less than 19.9% and relative error of the reconstructed total light source power are less than 1%. We observe a good agreement between the reconstructed values of the optical parameters, the light source power and their true values.

Despite the lack of a theoretical result on solution uniqueness, in the previous two examples, we obtain rather good numerical results. We owe this largely to the assumptions that the parameters D and μ are piecewise constants, and the regions where D and μ are piecewise constants are pre-determined.

5. Concluding remarks

In the conventional BLT problem, the optical parameters are assumed to be known exactly, and the only unknown is the light source function. Such a formulation has been theoretically studied in [12, 21]. We emphasize that in reality, the optical parameters are known only approximately. Thus, there is a need to estimate these parameters more accurately and improve the BLT reconstruction accordingly. In this paper, we have developed a novel framework integrating diffuse optical tomography (DOT) and conventional bioluminescence tomography (BLT) in a truly synergic fashion so that optical parameters are optimally estimated while an underlying bioluminescent source distribution is reconstructed. We have proved the existence of solutions to this generalized BLT problem and the convergence of the numerical solutions, as have been illustrated in our numerical simulation.

Finally, some comments on the uniqueness of the analytical and numerical solutions are in order. It is well known that in the general case the solution to the BLT problem is not unique unless adequate constraints are imposed such as when the solution is sought in a certain sense in a specified space. Similarly, we recognize that the solution to the upgraded BLT problem considered in this paper is not unique either but uniqueness may be achieved under sufficient

restrictions. In the BLT area, multi-spectral data were already utilized to overcome the ill-posed nature of BLT and generated encouraging results [4, 6, 9, 13, 14, 23]. Furthermore, temperature-modulated BLT was recently proposed to transform the ill-posed BLT problem into a much better conditioned problem [22]. Along these directions, our new BLT formulation may be extended for even better reconstruction results. Further work is currently underway.

Acknowledgments

This work was supported by NIH grants EB001685 and EB006036. The authors thank an Editorial Board member and two anonymous referees for their valuable comments.

References

[1] Arridge S R 1999 Optical tomography in medical imaging *Inverse Problems* **15** R41–R93
[2] Atkinson K and Han W 2005 *Theoretical Numerical Analysis: A Functional Analysis Framework* 2nd edn (New York: Springer)
[3] Brenner S C and Scott L R 2002 *The Mathematical Theory of Finite Element Methods* 2nd edn (New York: Springer)
[4] Chaudhari A J, Darvas F, Bading J R, Moats R A, Conti P S, Smith D J, Cherry S R and Leahy R M 2005 Hyperspectral and multispectral bioluminescence optical tomography for small animal imaging *Phys. Med. Biol.* **50** 5421–41
[5] Ciarlet P G 1978 *The Finite Element Method for Elliptic Problems* (Amsterdam: North-Holland)
[6] Cong A and Wang G 2006 Multi-spectral bioluminescence tomography: methodology and simulation *Int. J. Biomed. Imaging* **2006** (Article ID 57614)
[7] Cong W X *et al* 2005 A practical reconstruction method for bioluminescence tomography *Opt. Exp.* **13** 6756–71
[8] Contag C H and Ross B D 2002 It's not just about anatomy: *In vivo* bioluminescence imaging as an eyepiece into biology *J. Magn. Reson. Imaging* **16** 378–87
[9] Dehghani H, David S C, Jiang S, Pogue B W and Paulsen K D 2006 Spectrally-resolved bioluminescence optical tomography *Opt. Lett.* **31** 365–7
[10] Engl H W, Hanke M and Neubauer A 1996 *Regularization of Inverse Problems* (Dordrecht: Kluwer)
[11] Evans L C 1998 *Partial Differential Equations* (Providence, RI: American Mathematical Society)
[12] Han W, Cong W X and Wang G 2006 Mathematical theory and numerical analysis of bioluminescence tomography *Inverse Problems* **22** 1659–75
[13] Han W, Cong W X and Wang G 2006 Mathematical study and numerical simulation of multispectral bioluminescence tomography *Int. J. Biomed. Imaging* **2006** (Article ID 54390) 10 pages
[14] Han W and Wang G 2007 Theoretical and numerical analysis on multispectral bioluminescence tomography *IMA J. Appl. Math.* **72** 67–85
[15] Herschman H R 2003 Molecular imaging: Looking at problems, seeing solutions *Science* **302** 605–8
[16] Natterer F and Wübbeling F 2001 *Mathematical Methods in Image Reconstruction* (Philadelphia, PA: SIAM)
[17] Ntziachristos V *et al* 2002 Fluorescence molecular tomography resolves protease activity *in vivo Nat. Med.* **8** 757–61
[18] Rice B W *et al* 2001 *In vivo* imaging of light-emitting probes *J. Biomed. Opt.* **6** 432–40
[19] Tikhonov A N 1963 Regularization of incorrectly posed problems *Sov. Dokl.* **4** 1624–7
[20] Wang G *et al* 2003 Development of the first bioluminescent CT scanner *Radiology* **229** 566
[21] Wang G, Li Y and Jiang M 2004 Uniqueness theorems in bioluminescence tomography *Med. Phys.* **31** 2289–99
[22] Wang G, Shen H, Cong W X, Zhao S and Wei G 2006 Temperature-modulated bioluminescence tomography *Opt. Exp.* **14** 7852–71
[23] Wang G, Shen H, Kumar D, Qian X and Cong W X 2006 The first bioluminescence tomography system for simultaneous acquisition of multi-view and multi-spectral data *Int. J. Biomed. Imaging* **2006** (Article ID 58601) 8 pages
[24] Weissleder R and Ntziachristos V 2003 Shedding light onto live molecular targets *Nat. Med.* **9** 123–8